Fast & Furious: Detecting Stress with a Car Steering Wheel

Pablo E. Paredes
Computer Science Department
Stanford University
Stanford, USA
pparedes@stanford.edu

Francisco Ordoñez
Computer Science Department
USFQ
Quito, Ecuador
francisco.ordonez@estud.usfq.edu.ec

Wendy Ju
Information Science
Cornell Tech
New York, USA
wgj23@cornell.edu

James A. Landay
Computer Science Department
Stanford University
Stanford, USA
landay@stanford.edu

ABSTRACT
Stress affects the lives of millions of people every day. In-situ sensing could enable just-in-time stress management interventions. We present the first work to detect stress using the movements of a car's existing steering wheel. We extend prior work on PC peripherals and demonstrate that stress, expressed through muscle tension in the limbs, can be measured through the way we drive a car. We collected data in a driving simulator under controlled circumstances to vary the levels of induced stress, within subjects. We analyze angular displacement data to estimate coefficients related to muscle tension using an inverse filtering technique. We prove that the damped frequency of a mass spring damper model representing the arm is significantly higher during stress. Stress can be detected with only a few turns during driving. We validate these measures against a known stressor and calibrate our sensor against known stress measurements.

ACM Classification Keywords
H.5.m. Information Interfaces and Presentation (e.g. HCI): Miscellaneous

Author Keywords
Stress Management, Modeling, Stressor, Driving, Infrastructure Mediated Sensing, Stress Detection, Stress Measurement

INTRODUCTION
Stress response is an evolutionary mechanism that mobilizes body resources to help cope with daily challenges and life-threatening situations. While acute stress is the short-term response to a particular challenge (i.e., a stressor) [22], chronic stress is the longer-term response that may appear when experiencing extreme life experiences [37]. Both chronic stress and repetitive daily acute stress have been associated with a variety of patho-physiological risks such as cardiovascular disease and immune deficiencies, which can dramatically impair quality of life and shorten life expectancy [9].

Figure 1. Experimental setup: (left) Participant driving in the simulator; (upper right) street view; (lower right) steering wheel angular rotation signal: *right* turn (>0°), *left* turn (<0°).

This research explores the opportunistic sensing of daily stressors by detecting mental stress from the way we drive a car. We do not propose the use of traditional stress sensors, such as Electrocardiogram (ECG) or Electro-Dermal Activity (EDA), but we rather propose the development of a new opportunistic infrastructure-mediated sensor [33, 31]. We design this in-situ sensor by re-purposing existing infrastructure embedded in modern cars in order to enable a way to pervasively monitor and improve wellbeing and health [29]. We extend the work by Sun et al. [42] to focus on signals that may already capture the changes in muscle tension in the limbs. We propose that the fight or flight response to stress, which affects the trapezius

CHI 2018, April 21–26, 2018, Montreal, QC, Canada

 ISBN 978-1-4503-5620-6/18/04…$15.00
DOI: https://doi.org/10.1145/3173574.3174239

and other muscles activated with the motion of the upper limbs, can be extracted from the pattern of changes to the steering wheel angle.

Stress affects driving performance in two ways. On the one hand, it is a source of traffic accidents and road rage [11]. On the other hand, it can increase performance [25]. Having an in-situ sensor of stress in a car can support the design of on-the-road interventions for stress regulation. Monitoring stress continuously, without the need for the driver to wear any additional sensors can lead to more fine-grained models of stress, driving performance, and their interacting effects on each other, without introducing any user burden. Importantly, understanding on-the-road stress patterns can also be used to improve the quality of the commute itself, by informing the design of commute interventions (e.g., to promote work-life balance[7], mental and physical relaxation[32], mindfulness[30], and general psychological wellness[29]) and, in turn, potentially even increasing perceived quality of life [27].

There are other tools to measure stress, which could be use in conjunction with our technique. The most commonly used tool to measure stress continues to be self-reports, with a recent increase in the use of wearables [10, 2, 5]. Only highly motivated individuals answer survey questions about stress, or remember to wear a stress device after a few weeks. Furthermore, self-reporting in the car context is a less desirable approach, considering how the distracting nature of the reporting activity could both produce an unreliable measurement (given one's attention is not fully attending to it) and be a safety risk (taking focus off driving). An in-car stress sensor can guarantee, at a minimum, a couple of readings per day.

This paper extends the work from Sun, et al. [42] to demonstrate that the damped frequency of a second order mass spring damper (MSD) model can be effectively linked to muscle stiffness derived from mental stress. We performed a within-subjects study (N=25) counterbalancing calm and stress conditions. We carefully selected a driving circuit and stressors to avoid any alteration in driving that may not be due to mental stress only. Subjective measurements, ECG, and EDA information was obtained to validate the efficacy of the stressors. We used the data from the already existing angular sensors on the steering wheel of the driving simulator (see Figure 1). Our results confirm a significantly higher damped frequency, i.e., an increase in muscle stiffness, for the stress condition. We also prove that the results hold even for a decimated signal, indicating the feasibility of our approach in real-world setups, where it would be viable to leverage the low resolution sensors found in most modern vehicles.

BACKGROUND AND PRIOR WORK

In this section, we introduce fundamental work that explains the effects of stress on muscle tension, the ways one can measure these effects, and traditional stress measurements required to calibrate our new sensor.

Stress Measurement

Stress can be measured in two ways, via self reports or through physiological signals. Stress self-report (SSR) is usually measured through some variation of the widely used Perceived Stress Scale (PSS) [6, 38]. Usually, a simplified version with a single 10-item scale of stress is used in repeated measure studies.

The most accepted and traditional way to measure stress is by capturing a signal correlated with arousal, i.e., an activation of the Autonomic Nervous System (ANS). The most common metrics are heart rate variability (HRV) and electrodermal activity (EDA). HRV is a second-order metric derived from the reading of an electrocardiogram (ECG) wave and is a proxy for the variability of HR due to the respiratory sinus arrhythmia (RSA). RSA stimulates the vagus nerve, which is the main driver of the Autonomous Nervous System (ANS). The ANS has two main branches: the Sympathetic Nervous System (SNS) and the Parasympathetic Nervous System (PNS). While SNS activation is associated with the "fight or flight" stress response, where many organs are activated to overcome a particular challenge or threat, the PNS works antagonistically to maintain a stable functioning condition.

In general, higher HRV indicates a prevalence of the PNS over the SNS (i.e., a balanced/calmer state). HRV is commonly evaluated in the time-domain with the Root Mean Square of Subsequent Samples (RMSSD) or in the frequency-domain with the Low Frequency (LF) and High Frequency (HF) components. RMSSD represents short term variability and is inversely correlated with arousal. EDA, previously known as Galvanic Skin Response (GSR), is a measurement of skin conductance due to the activation of the eccrine sweat glands, which are only innervated by the SNS. High average levels and increased number of EDA peaks have been associated with stress [3].

Detecting Stress through its Musculoskeletal and Movement-Based Expressions

Mental stress has a direct effect in musculoskeletal activity. Muscle tension increases due to mental stress, even at rest [4, 8]. Tension in the forehead, the neck, and arms increases with stress and anxiety [41, 18]. Traditional lab stressors, such as mental arithmetic, have shown clear effects on the shoulder's trapezius muscle [23], as well as the biceps and triceps [44]. Driving experiments with on-road stressors have also revealed an increased level of muscle tension in the trapezius muscle captured by burdensome instruments infeasible for everyday use [13, 25].

To our understanding, there is no prior work on using the signal from the steering wheel to detect stress. Our work, however, extends prior work on stress detection and emotion through the use of computer peripherals. Sun, et al. were the first to show a direct effect of stress on the way a PC mouse is handled [42]. Their approach uses an inverse filtering technique, which directly correlates features from a second order oscillatory system back to the muscle tension. Other approaches have shown signals of stress in the way people hold a mouse and their typing pressure [16] or the way people swipe on touch devices [12]. As explained earlier, due to the lack of understanding of the effects of induced stress in drivers, this is the first study focused on obtaining lab data from a driving simulator. We captured data from a gaming steering wheel

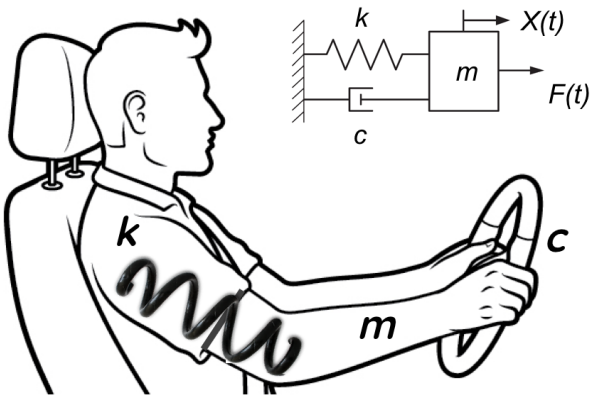

Figure 2. MSD model of the human arm while driving.

connected to a driving simulator running commercial driving school training software – see the *Apparatus* subsection for additional details.

MODELING THE HUMAN ARM WHILE DRIVING

In this work, we extend prior work on human arm modeling from PC peripherals to car driving tasks. We focus on modeling the human arm as it operates a simulator steering wheel.

Neuromuscular Dynamics

Prior work has successfully shown the use of a Mass Spring Damper (MSD) system to model a human arm while handling a steering wheel. Systems with a single degree of freedom [34] or two degrees of freedom [35] have been tested. The MSD is regularly used in modeling arm motion [17] in diverse tasks ranging from handwriting [19] to robotics [26] to assistive technology [39]. More recently Sun, et al. successfully modeled the arm as a single degree of freedom MSD system applied to interactions with computer peripherals [42]. In this work, they describe a MSD system applied to each direction of movement of a PC mouse.

In the single order MSD system, the *mass* component represents an aggregate sum of the arm, hand, and wheel. The *spring* component represent the muscle tension in the arm, while the *damper* represents muscular interaction in the arm and the damping effect of force feedback of the simulator steering wheel (see Figure 2). The input force *F(t)* of the arm produces an output movement *X(t)* in the steering wheel, measured in radians. A MSD responds with a oscillation frequency driven by the spring component (k) and a characteristic decay function determined by the friction of the damper component (c). This *damped oscillatory* behavior can be fully characterized by the *damped frequency* (ω) and the *damped ratio* (ζ). For a system with constant mass, the spring coefficient is *directly* proportional to the damped frequency: $\omega \approx \sqrt{k}$ and the damping ratio is *indirectly* proportional to the square-root of k while being directly proportional to c: $\zeta \approx \frac{c}{\sqrt{k}}$. These relationships show a direct relationship between muscle tension, caused by stress, and the MSD model.

Inverse Filtering

Since the steering wheel angle is the output signal of the MSD system, we have to apply an inverse filtering technique to infer the system's fundamental parameters. A successful technique used to model a single degree of freedom MSD is linear predictive coding (LPC). It is well-documented that an ideal second order system, such as the MSD, can be inferred via LPC using only two samples from the past [28]. Conversely, if we model a second order LPC we should be able to recover the characteristic MSD parameters.

MSD Computation

We use a logger that samples the steering wheel with a sampling period of about (M = 1.1, SD = 0.34) milliseconds. The wheel has a resolution of 0.0056° and a maximum range of 450° in each direction. Positive angle rotations are recorded when the wheel turns clockwise, i.e., when the car turns *right*, and negative angle rotations are recorded when the wheel turn counterclockwise, i.e., when the car turns *left*. The signal are interpolated with a shape preserving function, and resampled to obtain a uniformly sampled signal. The LPC model is calculated using an interpolation order of (p=4) to obtain a sequence of coefficients that can effectively model the underdamped MSD system. The complex *roots* (r) of this polynomial characterize the MSD's damping behavior. The absolute value of the imaginary part represents the damping frequency ($\omega = |\Im(r)|$), while the ratio of the real part to its absolute value represents the damping ratio ($\zeta = \frac{|\Re(r)|}{||r||}$).

METHOD

In this section, we outline our hypothesis, describe the experimental design, and detail our data collection methods.

Hypothesis

Based on the preliminary discussion we propose a single hypothesis:

(H): The damped frequency ω should be higher due to higher stress compared to a calm baseline.

In contrast to prior reports by Sun et al., we do not see merit in formulating a hypothesis around the damping ratio ζ, as we have no way to directly measure the damping effects of the steering wheel. Furthermore, a careful examination of their paper does not reveal a reduction in the damping ratio. This could be due to the effect of the damping coefficient of the arm muscles. We also do not evaluate turn completion *time* as a variable correlated with stress for two reasons: first, it is hard to truly evaluate the complete duration of a turn, and second, mental stress usually affects task completion, which in this case would be measured by lap completion, which is affected by changes in acceleration or speed, as opposed to the speed of turning.

Participants

We recruited 25 participants, 13 females and 12 males, with ages ranging from 18 to 67 (M = 34.43, SD = 15.05). Prior to participating in the experiment, we asked their preferred genre of music. We used their selection to find a playlist from

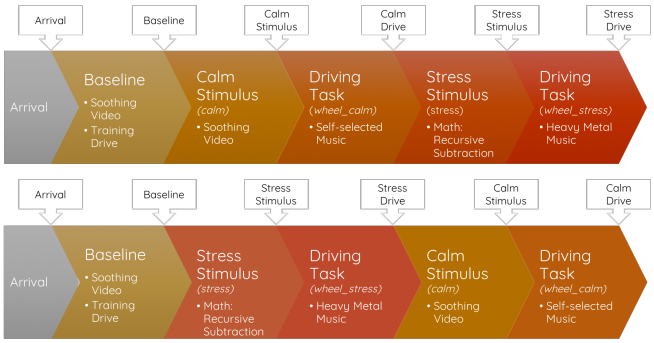

Figure 3. Experiment Procedure. Counterbalanced conditions: top) *Calm –> Stress*; bottom) *Stress –> Calm*

Spotify[1]. No participant reported liking heavy metal music, which we used in the stressor portion of our study.

Experiment Design

In this section, we describe the procedure, the driving task and the stressors for our experiment.

Testing Procedure

The experiment consisted of five stages: (1) Arrival, (2) Baseline: Soothing Video + Training Drive, (3) Stimulus 1, (4) Drive Task 1, (5) Stimulus 2, and (5) Drive Task 2. The first three stages lasted on average 3 minutes each, while the driving stages lasted 10 minutes on average. The *Arrival* stage was used to gather pre-test information. During the *Stimulus* stages, participants either received an acute stressor or a soothing intervention, as described in the *Stimulus* section. During the *Driving* task users received an exacerbating stressor to maintain the level of stress during the whole duration of the experiment and a relaxing stimulus to maintain a low level of stress. Calming and Stress stimulus + driving tasks were counterbalanced across participants (see Figure 3). We called each of the four different stimulus and driving conditions: *stress*, *calm*, *wheel_stress*, and *wheel_calm*.

Driving Task

The selection of the driving task is of crucial importance to isolate the effects of mental stress. Neither the task, nor the stressor, should alter the cognitive, attentive or performance responses. For this reason, the driving circuit had no traffic, pedestrian distractions, traffic symbols, or bumps. We chose a driving training circuit with 28 turns, 12 turns to the right and 16 to the left (see Figure 4). To record a minimum of turns, participants were asked to complete four laps around the circuit, for a total of 112 turns, and a minimum of at least 48 turns in each direction. Due to procedural errors, one participant completed only three laps while five participants completed five laps each. Participants were requested to drive as they would normally drive a vehicle in the city. Turns were mostly 90° turns with a radius of about 12 feet. There were no interruptions between turns. All drivers circulated around the lap in a counterclockwise direction. It is important to note that most participants made an effort to drive as they would normally drive a vehicle during the first half of the laps.

[1]http://spotify.com

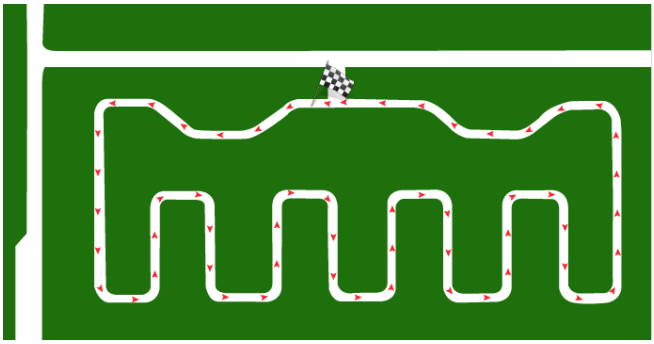

Figure 4. Driving circuit with 28 (16 left and 12 right) turns per lap. The circuit was traversed counterclockwise. The bright green dot indicates the starting point.

However, some participants, perhaps due to boredom, adopted more playful behavior towards the end, making more mistakes and being less precise in taking the turns.

Apparatus

The experiment was performed in a laboratory setting, using a half-car (buck) Skyline simulator setup [1] with a Logitech G29 gaming steering wheel and pedals[2] (see Figure 1). The car seat was positioned to a comfortable position, and sound effects were held constant. For the driving simulation environment, we used a commonly used driving school simulator, City Car Driving[3]. The data from the steering wheel was sampled at 916HZ with an angular resolution of 0.056°. This raw data was captured with a lossless computer logger that recorded the information directly from Logitech's steering wheel drivers.

Stimulus

The calming and stress conditions were each composed of two parts: An acute pre-driving stressor or soothing intervention coupled with arousing or soothing music, respectively, while driving (see Figure 3).

a. Pre-driving Stimulus. For the calming pre-driving stimulus, we had participants view a soothing video; this is recommended by other researchers as opposed to doing nothing to engender calm [36]. For the pre-driving acute stressor, we implemented a math stressor from the Trier Social Stress Test (TSST) [20]. The task involved participants performing a series of subtractions out loud (13 from 2017, 13 from 2014 and so forth). If the participant made a mistake, the researcher asked the participant to start again. To add more stress, we created penalties associated with long response times – if users took more than four seconds to respond, they had to start over. We refer to this stressor as *Math*.

b. Sustaining Stimulus. To capture enough data from driving, we had to ensure that the effect of the acute stressor would last during the four driving laps. During the driving tasks, participants heard either their self-selected music genre or heavy metal music. The latter is associated with increased

[2]http://gaming.logitech.com/en-us/product/g29-driving-force
[3]http://citycardriving.com

levels of arousal [21]. We used a medley of songs from the album "At the Heart of Winter" by Immortal[4].

Stress Data Acquisition & Processing

During the experiment, stress was measured through self-reports and physiological measurements. Self-report stress (SRS) measurements were obtained after using a simplified version of the Perceived Stress Scale (PSS) [38], a 10-point scale question: "What is your current level of stress?" with end points "Low" and "High" immediately after completion of each stage (see Figure 3). SRS was normalized and corrected against its baseline per participant to minimize potential individual differences. As ancillary self-reported metrics we asked the level of *Tension* from 0-"Low" to 10-"High", the level of *Concentration*, also with the same range, and the dual affective components: *Arousal* and *Valence*, based on Russell's affect circumplex [40]. As will be explained later in the stress evaluation section, these metrics, together with task performance analysis, were used to verify that our stressor did not induce changes that could not be attributed solely to mental stress.

An Electrocardiogram (ECG) signal ($250Hz$) was measured with the Zephyr BioModule Device 3.0[5]. The strap was wrapped around the participant's torso just under the chest area, so that the sensor unit was aligned with their left lateral side. HRV is a second-order metric derived from the ECG signal. HRV is evaluated by detecting the maximum peaks (R peaks) of the ECG signal. In the time-domain, HRV is commonly measured using the Root Mean Square of Subsequent Samples (RMSSD), which represents short term variability and is inversely correlated with arousal. R-peak detection of the ECG signal was manually examined following the recommendations of the HRV task force [43] using the Kubios software[6]. RMSSD was normalized and baseline-corrected per individual.

EDA, previously known as Galvanic Skin Response (GSR), is a measurement of skin conductance due to the activation of the eccrine sweat glands which are purely innervated by the SNS. High average levels and increased number of EDA peaks have been associated with stress [3]. EDA ($4Hz$) was measured with the Empatica E4 sensor[7]. The Empatica E4 band was wrapped around the participant's wrist of the non-dominant arm. The device was mounted to allow proper skin contact without restricting blood flow. The *Event Marking* feature of the Empatica device was used to record time stamps for both devices. Several processing steps were applied. First, exponential smoothing ($\alpha = 0.08$) was applied to reduce high-frequency artifacts due to motion. Second, each of the sessions was normalized between 0 and 1 [24] to amplify EDA changes and minimize daily differences due to sensor placement. Third, phasic EDA components were automatically extracted with the Ledalab library[8]. Finally, we extracted the average number of phasic peaks for each part of the experiment (see the Results section). The peaks were extracted with the FINDPEAKS function of MATLAB and were normalized for each session to be between 0 and 1 to further minimize session differences.

[4]https://www.youtube.com/watch?v=VeOlPQqJR-o
[5]https://www.zephyranywhere.com/
[6]http://www.kubios.com/
[7]https://www.empatica.com/
[8]http://www.ledalab.de/

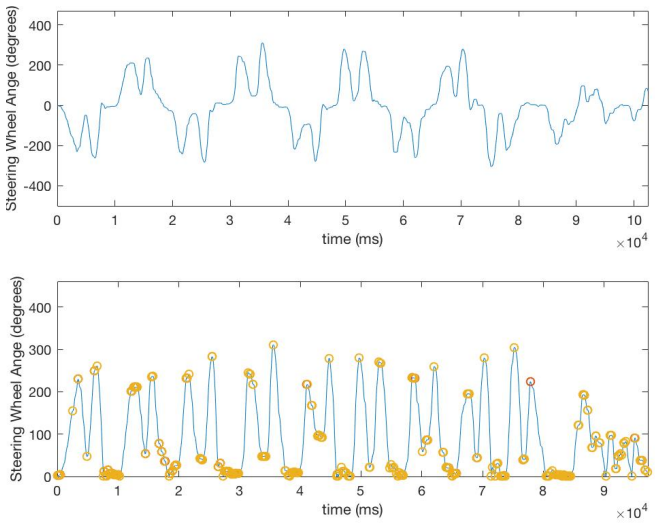

Figure 5. Turns. a) Excerpt of the original signal; b) Absolute value of the signal with peaks and valleys.

Steering Wheel Data Acquisition & Processing

Data acquisition and preprocessing were performed to create a signal viable for analysis with a linear predictive coding technique.

Preprocessing

Several steps were followed to process the steering wheel signal. First, we eliminated repeated timestamps, which accounted for about 9.69% of the samples. After this, the signal was filtered to eliminate high frequency components. We used a 20 pole Butterworth low-pass filter with a cutoff frequency of $\omega = 0.2 * \pi$ *rad/sample*. We then interpolated the signal to correct the original sampling period τ = (M = 1.0918, SD = 0.5179) *ms* to have a uniformly sampled signal τ = (M = 1, SD = 0) *ms*.

Segmentation

To extract valuable data segments, several assumptions were made based on exploratory analysis of the signal. First, the data was transformed from a +/- 450° signal into its absolute value (0 to 450°). This way, all positive "peaks" represented either right or left turns (see Figure 5).

We decided to use only monotonically increasing segments, since they represent direct activation of the muscles. Although the monotonically decreasing segments could carry some signal from the muscle, it can also carry some of the effect of the steering wheel's force-feedback mechanism. Furthermore, in real-life settings the steering wheel return path is also many times strongly guided by the force of the wheels returning to their initial position. To discover these segments we used the FINDPEAKS function from Matlab to find the signal's peaks and valleys. We extracted all segments between a valley and a peak (in that order).

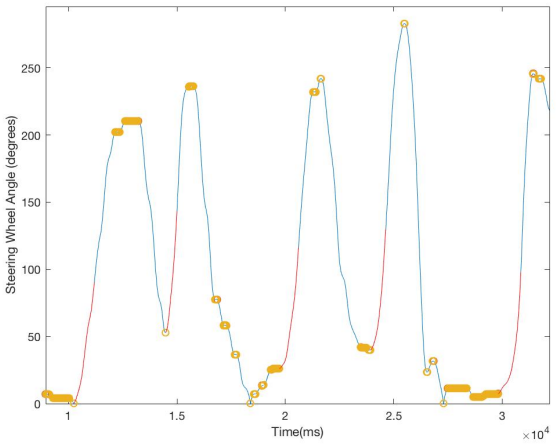

Figure 6. Detail of a couple of steering wheel turns. Extracted segments marked in red.

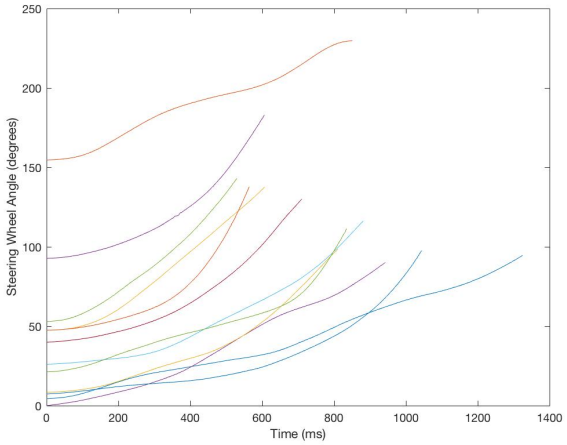

Figure 7. Some sample segments from participant P2's *calm* driving condition.

To capture the activation of the arm and shoulder, rather than small movements from the forearm only, we decided to eliminate segments that are smaller than 40°. As observed in Figure 5, most of the turns are larger than this value. On the other end of the range, most turns were at most 280°to 320°. We did not include turns larger than that, as they could have been done in a hurry, perhaps trying to take a rapid turn to correct for some mistake. One final observation of the data showed that for larger turns, around 90° there seemed to be a secondary "impulse." We decided to truncate these turns to keep only the "first" muscle impulse, to avoid readings that may be confounded by the existing inertia of the turn. In summary, we decided to pick turns that were larger than 40°, but smaller than 320°, and we truncated turns larger than 90 degrees (see Figure 6).

We acknowledge that these meta parameters could be further validated with a more detailed study of the activation of the arm muscles with either EMG sensors or motion capture cameras. We did a quick observational run with a male and a female driver to see if our parameters were minimally acceptable. We asked the drivers to drive around the city and report when they felt that the whole arm was activated. They reported that the arm was active when taking turns that were about 45°to 70°. Smaller turns seemed to be performed by using the arm's weight or just wrist or forearm activation only. The users reported feeling that their arm was fully engaged for up to 90°to 180°, which was close to our observation of a secondary "impulse" happening around 90°to 120°.

We felt that our meta parameters were conservative and realistic enough to capture the desired movement activation. During *wheel_calm*, we obtained (M = 22.92, SD = 10.12) segments per participant per lap with an average duration per segment of (M = 748.75 SD = 152.98) *ms* and for *wheel_stress* we obtained (M = 23.48, SD = 7.12) segments with a duration of (M = 658.70, SD = 163.30) *ms* for the *wheel_stress* condition. On average, we obtained 23.2 turns, which represent roughly 83% of the 28 actual turns of our driving circuit. Figure 7 shows a few turn segment samples from the *calm* condition for participant P2. Most of the samples show an exponentially accelerating curve, characteristic of an under-damped oscillatory system.

Pole Selection

Finally, the selected segments were processed with a fourth order linear predictor coding (LPC) algorithm. This configuration generates a representation of a second order MSD system. We focused on extracting only the under-damped poles, i.e., those with an imaginary part larger than 0. By picking the under-damped poles we retained 88.34% of the total segments per user in the *wheel_calm* condition and 89.94% of the total segments per user in the *wheel_stress* condition. As explained in the modeling section, under-damped poles have a direct relationship with the k coefficient of a MSD system representing the human arm.

RESULTS

In this section, we present the validation of both the stressor with self-reported and physiological measurements, and the model, which is derived from steering wheel measurements.

Stress Evaluation

First, we validate that our stressor only elicits mental stress by discarding the effect of *concentration* or *task performance* artifacts. Then, we present self-reported and physiological measurements that prove the efficacy of our stressor.

Mental stress validation

We start by confirming that the movement response to our stressors was not contaminated by movements that may be caused by other cognitive processes. Specifically, we controlled for concentration effects and task-related performance. We analyzed two metrics: perceived *concentration* and *lap duration*. First we averaged *concentration* levels before and after the driving conditions. No difference was found between *wheel_calm* (M = -0.344, SD = 0.324) and *wheel_stress* (M = -0.323.519, SD = 0.371) ($t(48)$ = 0.223, p = 0.824). *Lap duration*, defined as the time to complete a complete lap around the

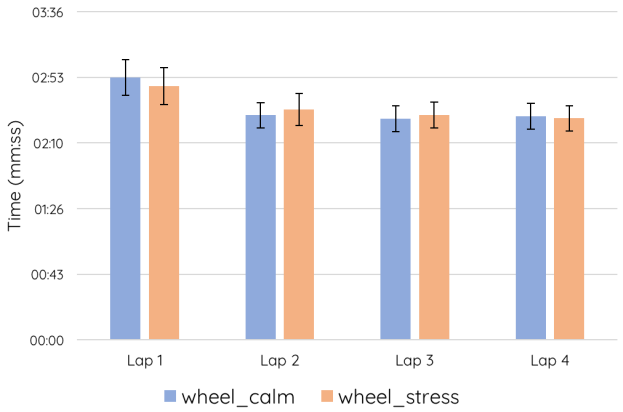

Figure 8. Lap duration in mm:ss. Error bars represent standard errors.

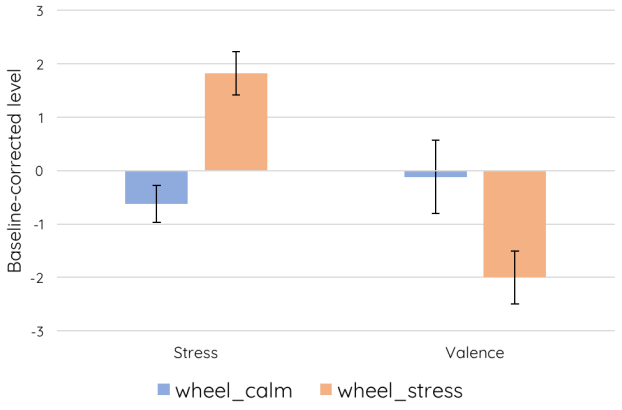

Figure 9. Perceived levels (baseline corrected) for Self-Reported Stress (SRS) and Valence. Error bars represent standard errors.

driving circuit, which could be affected by an intrinsic or extrinsic motivation, also did not show a difference between the *wheel_calm* ($M = 2.33$, $SD = 0.45$) and *wheel_stress* ($M = 2.34$, $SD = 0.33$) states ($t(48) = -0.0466$, $p = 0.963$). Furthermore, no differences were observed in pairwise *lap duration* comparisons (see Figure 8). Finally, we tested the difference in time duration across the turn segments. Again, we found no significant difference between the *wheel_stress* and *wheel_calm* states. These results ensure us that our *math+heavy metal music* stressor produced mainly changes in mental stress rather than in task-related *concentration* or *performance*, which in turn should affect muscle tension in the upper limbs.

Self-reported Metrics

To correct for individual differences we used the change with respect to individual baselines as our analysis metric. For self-reported stress (SRS), we found a significant difference between *wheel_calm* ($M = -0.62$, $SD = 1.728$) and *wheel_stress* ($M = 1.82$, $SD = 2.046$) ($t(48) = 9.956$, $p < 0.001$). As expected, *SRS* was higher in the presence of stress (see Figure 9 - Self-Report). In addition to *SRS*, we found that *Tension* was significantly higher for *wheel_stress* (M=-1.22, SD=2.092) than for *wheel_calm* (M=1.12, SD=1.878) ($t(48)$=4.162, $p <$ 0.001). Furthermore, perceived tension and stress were highly correlated ($r = 0.686$, $p < 0.001$), which indicates a perceived relationship between stress and muscle tension.

We did not find a significant difference for *Arousal/Energy*, however, *Valence/Feelings* was significantly lower for *wheel_stress* (M=-0.12, SD=3.441) than for *wheel_calm* (M=-2, SD=2.483) ($t(48)$=-2.215, $p < 0.05$). The latter result indicates that people perceived our stressor as "distressing" rather than a neutral challenge. These ancillary metrics support the notion that we were successful in inducing stress (distress) during our experiment (see Figure 9).

Physiological Stress

We normalized all physiological metrics per user including baseline values to control for individual differences. For *RMSSD*, we observed a significant difference between the calm and stressful stimulus *calm stimulus* ($M = 0.664$, $SD =$ 0.401) and *stress stimulus* ($M = 0.293$, $SD = 0.508$) ($t(48) = -3.562$, $p < 0.01$) (see Table 1). As expected, *RMSSD* was lower in the presence of stress. Furthermore, we found a significant difference for *mean HR* between *calm stimulus* ($M = 0.135$, $SD = 0.278$) and *stress stimulus* ($M = 0.857$, $SD = 0.289$) ($t(48) = 8.602$, $p < 0.001$) (see Table 1). We did not find differences in any *EDA* metrics between the calm and stress stimulus.

When comparing the driving segments, we did not find a significant difference for either *RMSSD*, *mean HR* or *EDA* (see Table 1). However, when looking at the first minute of driving (10% of the data), we found that *EDA Phasic* was significantly different between *wheel_calm* ($M = 0.121$, $SD = 0.207$) and and *wheel_stress* ($M = 0.34$, $SD = 0.332$) ($t(48) = 2.795$, $p < 0.01$). We also found a statistically significant difference between *mean HR wheel_calm* ($M = 0.585$, $SD =$ 0.313) and *wheel_stress* ($M = 0.343$, $SD = 0.337$) ($t(48) =$ -3.021, $p < 0.01$). However, this change is non intuitive, as *mean HR* seems to be lower during the stress phase. These findings seem to indicate that physiological sensors fail to capture residual perceived stress while driving. Later, in the sensitivity evaluation subsection we present a lap analysis to further analyze the differences between our sensor and traditional physiological metrics.

Stress Steering Wheel Sensor Test

As previously described, we want to verify if the angular movement of a steering wheel can be used to model an approximation of a mass-spring damper model (MSD) of the human arm. We expect that the spring coefficient k representing muscle stiffness increases with stress. We use an inverse coding technique, linear predictive coding (LPC), to estimate the damped frequency of the MSD, which is proportional to the spring constant $\omega \approx \sqrt{k}$.

Measurement	Stimulus conditions			Driving conditions			
	Calm	*Stress*	*Stress-Calm*	*wheel_calm*	*wheel_stress*	*Full circuit*	*1st. minute*
	Mean (SD)	*Mean (SD)*	*t(48)*	*Mean (SD)*	*Mean (SD)*	*t(48)*	*t(48)*
RMSSD	0.664 (0.4)	0.293 (0.295)	-3.562**	0.316 (0.335)	0.336 (0.295)	0.203, 0.84	1.287
Mean HR	0.135 (0.278)	0.857 (0.289)	8.602**	0.574 (0.289)	0.554 (0.312)	-0.096	-3.021**
EDA Peaks	0.153 (0.249)	0.103 (0.151)	-0.861	0.785 (0.206)	0.794 (0.241)	0.146	-1.988
EDA Phasic	0.53 (0.388)	0.518 (0.377)	-0.113	0.297 (0.331)	0.366 (0.465)	0.602	2.795**

Table 1. Physiological measurements for stimulus and driving conditions. *p<0.05, **p<0.01

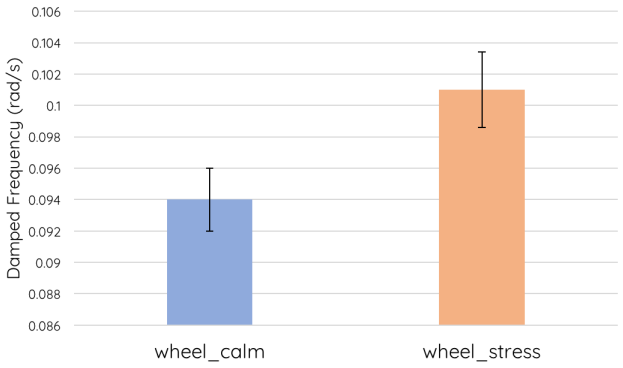

Figure 10. Damped natural frequency *(rad/s)* for *wheel_calm* ωc and *wheel_stress* ωs. Error bars represent standard errors.

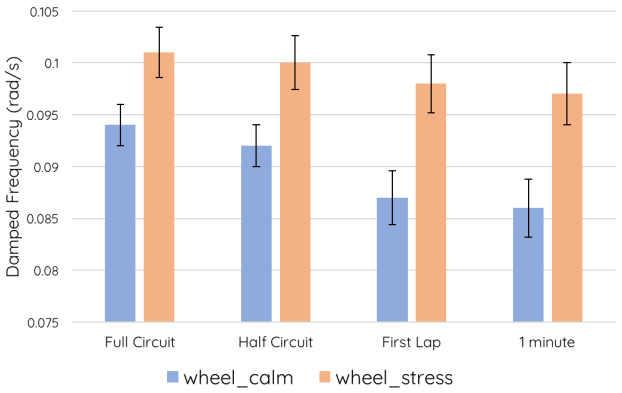

Figure 11. Reduction in number of laps (sample size). Error bars represent standard errors.

We define ωc and ωs as the damped frequency for all users' turn segments in the *wheel_calm* and *wheel_stress* conditions, respectively. ω values will always be measured in *rad/s*. We tested the entire dataset: 4 laps, (M=10:07, SD=3.05) minutes which includes (M = 96.12, SD = 27.12) turn segments per participant. ωs (M = 0.101, SD = 0.012) was found to be significantly higher than ωc (M = 0.094, SD = 0.01) (t = (48) = 2.053, p = <0.05) (see Figure 10). This result rejects the null hypothesis for H and implies that ω was able to effectively represent the muscle stiffness of the arm. We have successfully shown, for the first time, that it is possible to use the angular displacement of the steering wheel as an effective instrument to detect mental stress.

Sensitivity evaluation

With encouraging results, we proceeded to explore the sensitivity of our sensor. We explored the sensitivity of the sensor with less data to determine the minimum amount of data for it to still effectively sense mental stress. First, we reduced the sample size and then we decimated the sampling rate to ensure these techniques would work in existing vehicles.

Sample Size & Lap analysis

First we looked at the first half of the data, two laps (M = 5:20, SD = 1.45) minutes, accounting for 52.15% of the data and (M = 47.2, SD = 14.9) valid turn segments per participant, some being discarded during the segment preprocessing phase (see the *Segmentation* subsection in the prior section). We found ωs (M = 0.1, SD = 0.013) to be significantly higher than ωc (M = 0.092, SD = 0.01) (t(48) = 2.23, p < 0.05). This difference, slightly higher than the difference with 100% of the data could be due to a higher effect of the *math* stressor during the earlier part of the drive. With just a single lap (M = 2:50, SD = 0:59) minutes, representing 28% of the data and only (M = 23.2, SD = 8.66) turn segments per participant, ωs (M = 0.098, SD = 0.014) was still significantly higher than ωc (M = 0.089, SD = 0.013) (t(48) = 2.541, p < 0.05). Finally, to our surprise, with only 10% of the signal (1 minute on average) and just (M = 7.54, SD = 3.52) turn segments per participant, ωs (M = 0.097, SD = 0.015) remained significantly higher than ωc (M = 0.086, SD = 0.014) (t(48) = 2.67, p < 0.05) (see Figure 11). We did not find a viable difference with only 5% of the signal. Our sensitivity analysis reveals an encouraging possibility to detect mental stress with just a few maneuvers of a steering wheel during an urban drive (Table 2).

	Sample Size		**Difference $\omega s - \omega c$**
# of laps	*time(mm:ss)*	*# of turn segments*	*Mean(SD) (rad/s)*
2 laps	5:20	47	0.008(0.01)*
1 lap	2:50	23	0.011(0.016)*
<1 lap	1:01	8	0.011(0.02)*

Table 2. Effect of the reduction in the number of laps on the difference between *wheel_stress* and *wheel_calm* ($\omega s - \omega c$). *p<0.05

As can be observed in Figure 11, the effect of stress is more noticeably changing in *wheel_calm* than in *wheel_stress*. This means that, as discussed earlier, there was a sheer effect of stress by driving, which makes is less probable to detect a difference in ω as time passes by and the effect of the initial stressor diminishes. Despite producing a significant difference, the sensitivity for 1 minute seems to have a larger standard deviation, which may indicate that a safe sample size would be between 8 and 23 samples. Additional testing would be needed to further characterize the lower limits of our sensor.

Sensor benchmark

We contrasted the lap sensitivity results with a similar analysis performed on physiological metrics. As seen in Table 3 only HR and EDA present significant differences for the early part of the driving task (around 1 minute, or 10% of the task), with HR presenting non-intuitive results. This analysis shows the potential our sensor has to differentiate lasting changes in muscle tension due to mental stress, as opposed to traditional sensors that seem to react well only under acute changes.

Stress Sensors	**Sample size**			
Stress - Calm Mean(SD))	*4 laps*	*2 laps*	*1 lap*	*<1 lap*
RMSSD (Norm.)	0.02(0.38)	0.023(0.454)	0.058(0.504)	0.139(0.593)
HR (Norm.)	-0.02(0.381)	-0.057(0.305)	-0.098(0.29)	-0.242(0.405)**
EDA Peaks (Norm.)	0.009(0.166)	0.014(0.132)	-0.02(0.067)	-0.011(0.03)
EDA Phasic (Norm.)	0.069(0.706)	0.116(0.478)	0.147(0.581)	0.218(0.377)**
WHEEL (rad/s)	0.006(0.009)*	0.008(0.01)*	0.011(0.016)*	0.011(0.02)*

Table 3. Sensor benchmark on the difference between *wheel_stress* and *wheel_calm* (ωs - ωc) for different sample sizes. *p<0.05, **p<0.01

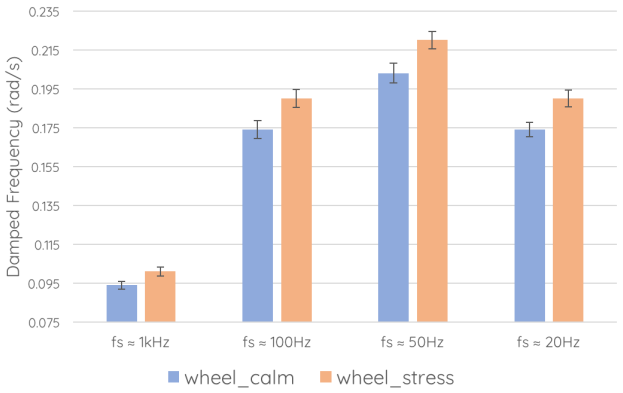

Figure 12. Sampling frequency decimation on data from a single lap. Error bars represent standard errors.

Sample Size	**Decimation Factor**		
1 lap, ≈2:50 min, ≈23 segments	*10*	*20*	*50*
$\omega s - \omega c$ Mean (SD) (rad/s)	0.017 (0.024)*	0.017 (0.026)*	0.014 (0.023)*

Table 4. Effect of decimation on the difference between *wheel_stress* and *wheel_calm* (ωs - ωc). *p<0.05

Decimation

To test if our findings still hold with a smaller sampling frequency (*fs*) and lower angular resolution (*ar*), similar to those found in consumer electronics On-Board-Diagnostics (OBD) devices[9], we lowered our sampling frequency by effects of signal decimation. On average consumer-end OBD devices sample rates are between 25 to 50Hz. Raw internal sampling rates range between 50 or 100Hz . In this paper we picked decimation factors of 10, 20 and 50. We performed this analysis using the single lap results, which showed a higher difference between ωs and ωc than the entire dataset (see Table 4).

With a decimation factor of 10 ($fs \approx$ 100Hz and $ar = 0.56°$), we observe that ωs ($M = 0.191$, $SD = 0.023$) is significantly higher than ωc ($M = 0.174$, $SD = 0.023$) ($t(48) = 2.572$, $p < 0.05$). With a decimation factor of 20 ($fs \approx$ 50Hz and $ar = 1.12°$), ωs ($M = 0.22$, $SD = 0.022$) was still significantly higher than ωc ($M = 0.203$, $SD = 0.025$) ($t(48) = 2.563$, $p < 0.05$). Surprisingly, with a decimation factor of 50, ($fs \approx$ 20Hz and $ar = 2.8°$), we still found that ωs ($M = 0.244$, $SD = 0.022$) was significantly higher than ωc ($M = 0.23$, $SD = 0.019$) ($t(48) = 2.41$, $p < 0.05$). A decimation factor of 100 did not render a significant difference. These results indicate that it is still possible to detect stress with a lower sampling frequency and lower resolution. It seems that the best sampling frequency is around 50Hz, as it has a stronger difference between the calm and stress conditions (see Figure 12). This is quite relevant, as it opens the possibility to use a wide variety of commercial OBD devices commonly used to extract information such as the angular variation of the steering wheel at low frequency.

Overall these encouraging sensitivity findings suggest that our sensor could potentially be used to monitor acute stress fluctuations during almost any common driving task within a city. A fine grained analysis with larger amounts of data and different driving scenarios should be performed to further evolve the understanding of the steering wheel stress sensor.

[9]https://en.wikipedia.org/wiki/On-board_diagnostics

DISCUSSION

This work represents the first successful use of a simulator steering wheel as a stress sensor. We were able to successfully induce stress during a driving task using *math* and without altering performance or driving mechanics. Furthermore, we were able to sustain the effects of stress and calmness with *music*, despite a natural tendency by drivers to get stressed while driving [14, 25]. We were successful at detecting the difference of our mental stressor through the muscle tension in the arm only using the angular displacement of the steering wheel. Furthermore, we showed significant results with as low as eight segments and with a decimated sampling frequency equivalent to 20Hz.

Applications

The sensor we have developed requires no new investment of hardware as it only requires signal processing of existing steering wheel angle signals already collected by the vehicle. We believe it would be easy to integrate our sensor into commercial passenger vehicles, thus converting modern cars into effective sensors for chronic and acute stress episodes.

After proving initial feasibility in the lab, substantial work must be made to extend this work to real world scenarios. Performance and sensitivity analysis on the road must be complemented with benchmarking other sensors. Some of the key challenges on the road would be related to the way people handle the steering wheel, such as single handed, double handed, etc. Power-steering and semi-automatic steering guidance technologies could interfere in the reading of the muscle tension. Road vibration could add additional noise that should be treated and removed before performing linear predictive coding or similar projective techniques. Finally, the actual task of driving in a real world setting could have a different mental effect on users, who may find themselves already in a stressful situation, and therefore make it difficult to differentiate acute from constant stress. We plan a series of further lab and road studies to explore the relationship between stress and acceleration, speed, road conditions, driver's abilities, power steering dampers' effects, and even relationships with signals from lower limbs, i.e., the accelerator and pedal angles.

It is worthwhile noting that this current work can already be used directly in car simulators, both for educational and gaming purposes. For example, the exact setup of our experiment, a Logitech G29 steering wheel coupled with the City Car Driving application, is a common driving simulation setup for people learning to drive. Gamers at different levels of proficiency could benefit from a steering wheel that reads stress or simply arousal levels. As a matter of fact, a range of games, from simple fun games such as Mario Kart, all the way to complex racing games such as Forza or Grand Theft Auto, could benefit from controls or challenges associated with the stress level of the user.

Looking at individual differences (see Figure 13), we observe that the majority of the participants showed an increase in

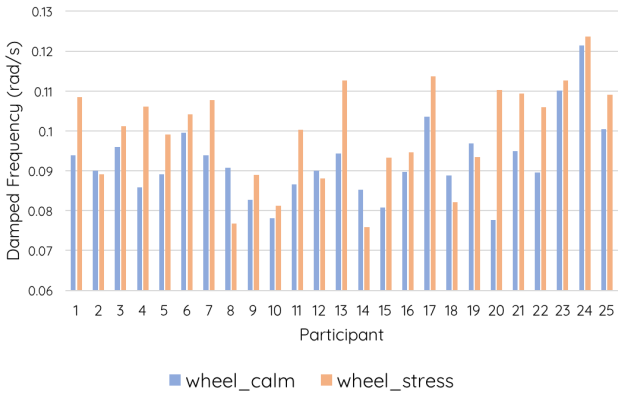

Figure 13. Individual differences for damped natural frequency *(rad/s)* observed after 2 laps (5:20 minutes).

damped frequency with stress, while only 5 of 25 experienced a decrease. Longitudinal evaluations of commuters or other drivers using cars on a daily basis would enable a deeper understanding of these individual differences.

Next steps

The stressor applied in this experiment, designed to elicit only mental stress as opposed to other cognitive alterations, was effective. However, it was also useful to learn that, despite increased stress levels, people did not have serious incidents while driving in the simulator. Therefore, we believe it is safe to advance this research to testing stress in real vehicles. We propose first controlled studies in closed circuits without actual traffic; in essence, a real-life version of our experiment. Real-driving scenarios should provide additional information of the effects of road-vibration and wheel mass inertia on the steering wheel stress sensor.

We are confident our technology could be adapted to commercial vehicles and further integrated with other stress sensors such as cameras or capacitive sensors in car seats. However, a key question remains: what to do when stress is detected? The fact that stress can be sampled at a relatively high rate means that this sensor could be used as input to interventions for commuters who may be stressed out from work, to help people manage road rage, or to simply make driving more enjoyable. If the goal is for these unobtrusive sensors to provide effective feedback about stress, complementary work on just-in-time interventions should be developed. Recently, Paredes et al. have suggested that when stress occurs during a drive, some plausible options could be to stretch or conduct breathing exercises [30, 32]. Others have suggested the use of wearables such as Moodwings [25], or light or sound displays such as Autoemotive [15] as ambient and peripheral feedback interventions.

CONCLUSION

In this paper, we have introduced a simple yet effective way to measure mental stress using only the steering wheel of an automobile. We have shown the efficacy of using a simple mass spring damper (MSD) model to detect the stress affecting the muscles of the arm. We calibrated our sensing algorithm against well known stress measurements such as self-reports, heart rate variability (RMSSD), and electrodermal activity (EDA). To validate our model, we have compared the damping frequency of the MSD system with well known math and music stressors. Using this model, we have found that it is possible to detect viable signals of stress with only a few turns, and that our sensor can capture longer term effects of stress expressed through muscle tension. This is the first work of this type, opening up new opportunities to use devices already embedded in a car as in-situ non-obtrusive stress sensors.

ACKNOWLEDGEMENTS

This work occurred under our institution's IRB # 37663. Toyota Research Institute ("TRI") provided funds to assist the authors with their research, but this article solely reflects the opinions and conclusions of its authors and not TRI or any other Toyota entity.

REFERENCES

1. Ignacio Alvarez, Laura Rumbel, and Robert Adams. 2015. Skyline: a rapid prototyping driving simulator for user experience. In *Proceedings of the 7th International Conference on Automotive User Interfaces and Interactive Vehicular Applications*. ACM, 101–108.
2. Urs Anliker, Jamie A. Ward, Paul Lukowicz, Gerhard Tröster, Francois Dolveck, Michel Baer, Fatou Keita, Eran B. Schenker, Fabrizio Catarsi, Luca Coluccini, Andrea Belardinelli, Dror Shklarski, Menachem Alon, Etienne Hirt, Rolf Schmid, and Milica Vuskovic. 2004. AMON: A wearable multiparameter medical monitoring and alert system. *IEEE Transactions on Information Technology in Biomedicine* 8, 4 (2004), 415–427. DOI: http://dx.doi.org/10.1109/TITB.2004.837888
3. Wolfram Boucsein. 1992. Electrodermal activity. *Electrodermal Activity* 3 (1992), 3–67. DOI: http://dx.doi.org/10.1007/978-1-4614-1126-0
4. John T. Cacioppo and Louis G. Tassinary. 1990. Inferring psychological significance from physiological signals. *American Psychologist* 45, 1 (1990), 16–28. DOI: http://dx.doi.org/10.1037/0003-066X.45.1.16
5. Jongyoon Choi, Beena Ahmed, and Ricardo Gutierrez-Osuna. 2012. Development and evaluation of an ambulatory stress monitor based on wearable sensors. *IEEE Transactions on Information Technology in Biomedicine* 16, 2 (2012), 279–286. DOI: http://dx.doi.org/10.1109/TITB.2011.2169804
6. Sheldon Cohen, Tom Kamarck, and Robin Mermelstein. 1983. A Global Measure of Perceived Stress. *Journal of Health and Social Behavior* 24, 4 (1983), 385. DOI: http://dx.doi.org/10.2307/2136404
7. Anna L. Cox, Jon Bird, Natasha Mauthner, Susan Dray, Anicia Peters, and Emily Collins. 2014. Socio-technical practices and work-home boundaries. In *Proceedings of the 16th ACM International Conference on Human-Computer Interaction with Mobile Devices & Services - MobileHCI '14*. 581–584. DOI: http://dx.doi.org/10.1145/2628363.2634259

8. Martha Davis, Elizabeth Robbins Eshelman, and Matthew McKay. 1988. *The Relaxation and Stress Reduction Workbook*. Vol. 331. 312–312 pages. DOI: http://dx.doi.org/10.1038/331312b0
9. Elissa S. Epel, Elizabeth H. Blackburn, Jue Lin, Firdaus S. Dhabhar, Nancy E. Adler, Jason D. Morrow, and Richard M. Cawthon. 2004. Accelerated telomere shortening in response to life stress. *Proceedings of the National Academy of Sciences of the United States of America* 101, 49 (2004), 17312–5. DOI: http://dx.doi.org/10.1073/pnas.0407162101
10. Emre Ertin, Nathan Stohs, Santosh Kumar, Andrew Raij, Mustafa al'Absi, and Siddharth Shah. 2011. AutoSense: unobtrusively wearable sensor suite for inferring the onset, causality, and consequences of stress in the field. In *Proceedings of the 9th ACM Conference on Embedded Networked Sensor Systems*. ACM, 274–287.
11. Tara E. Galovski and Edward B. Blanchard. 2004. Road rage: A domain for psychological intervention? (2004). DOI:http://dx.doi.org/10.1016/S1359-1789(02)00118-0
12. Yuan Gao, Nadia Bianchi-Berthouze, and Hongying Meng. 2012. What Does Touch Tell Us about Emotions in Touchscreen-Based Gameplay? *ACM Transactions on Computer-Human Interaction* 19, 4 (2012), 1–30. DOI: http://dx.doi.org/10.1145/2395131.2395138
13. Jennifer Healey, Justin Seger, and Rosalind Picard. 1999. Quantifying driver stress: Developing a system for collecting and processing bio-metric signals in natural situations. In *Biomedical Sciences Instrumentation*, Vol. 35. 193–198.
14. Jennifer A. Healey. 2008. Sensing Affective Experience. In *Probing Experience*. 91–100. DOI: http://dx.doi.org/10.1007/978-1-4020-6593-4{_}8
15. Javier Hernandez, Daniel McDuff, Xavier Benavides, Judith Amores, Pattie Maes, and Rosalind Picard. 2014a. AutoEmotive: Bringing Empathy to the Driving Experience to Manage Stress. *Proceedings of the 2014 companion publication on Designing interactive systems - DIS Companion '14* (2014), 53–56. DOI: http://dx.doi.org/10.1145/2598784.2602780
16. Javier Hernandez, Pablo E. Paredes, Asta Roseway, and Mary Czerwinski. 2014b. Under pressure: Sensing stress of computer users. In *Proceedings of the ACM SIGCHI Conference on Human Factors in Computing Systems - CHI 2014*. 51–60. DOI: http://dx.doi.org/10.1145/2556288.2557165
17. A. V. Hill. 1938. The Heat of Shortening and the Dynamic Constants of Muscle. *Proceedings of the Royal Society B: Biological Sciences* 126, 843 (1938), 136–195. DOI:http://dx.doi.org/10.1098/rspb.1938.0050
18. Rudolf Hoehn-Saric and Daniel R. McLeod. 1993. Somatic manifestations of normal and pathological anxiety. In *Biology of Anxiety Disorders*. 177–222. http://ezproxy.net.ucf.edu/login?url=http://search.ebscohost.com/login.aspx?direct=true&db=psyh&AN=1993-97167-005&site=ehost-live
19. John M. Hollerbach. 1981. An oscillation theory of handwriting. *Biological Cybernetics* 39, 2 (1981), 139–156. DOI:http://dx.doi.org/10.1007/BF00336740
20. Clemens Kirschbaum, K-M Pirke, and Dirk H. Hellhammer. 1993. The 'Trier Social Stress Test'–a tool for investigating psychobiological stress responses in a laboratory setting. *Neuropsychobiology* 28, 1-2 (1993), 76–81. DOI:http://dx.doi.org/119004
21. Elise Labbé, Nicholas Schmidt, Jonathan Babin, and Martha Pharr. 2007. Coping with Stress: The Effectiveness of Different Types of Music. *Applied Psychophysiology and Biofeedback* 32, 3-4 (2007), 163–168. DOI: http://dx.doi.org/10.1007/s10484-007-9043-9
22. Richard S. Lazarus. 1966. *Psychological Stress and the Coping Process* (print book ed.). New York: McGrawHill series in psychology. xiii, 466 pages.
23. Ulf Lundberg, Roland Kadefors, Bo Melin, Gunnar Palmerud, Peter Hassm6n, Uif Lundberg, Peter Hassmén, and Margareta Engström. 1994. Psychophysiological Stress and EMG Activity of the Trapezius Muscle. *International Journal of Behavioral Medicine* (1994), 354–370. DOI: http://dx.doi.org/10.1207/s15327558ijbm0104{_}5
24. David T. Lykken and Peter H. Venables. 1971. Direct measurement of skin conductance: A proposal for standardization. *Psychophysiology* 8, 5 (1971), 656–672. DOI: http://dx.doi.org/10.1111/j.1469-8986.1971.tb00501.x
25. Diana MacLean, Asta Roseway, and Mary Czerwinski. 2013. MoodWings - A Wearable Biofeedback Device for Real-Time Stress Intervention. *Proceedings of the 6th International Conference on Pervasive Technologies Related to Assistive Environments - PETRA '13* (2013), 1–8. DOI:http://dx.doi.org/10.1145/2504335.2504406
26. Thomas H. Massie and J. K. Salisbury. 1994. The PHANTOM Haptic Interface : A Device for Probing Virtual Objects. *ASME Winter Annual Meeting, Symposium on Haptic Interfaces for Virtual Environment and Teleoperator Systems* 55 (1994), 1–6. DOI: http://dx.doi.org/10.1145/1029632.1029682
27. Lars E. Olsson, Tommy Gärling, Dick Ettema, Margareta Friman, and Satoshi Fujii. 2013. Happiness and Satisfaction with Work Commute. *Social Indicators Research* 111, 1 (2013), 255–263. DOI: http://dx.doi.org/10.1007/s11205-012-0003-2
28. D. O'Shaughnessy. 1988. Linear predictive coding. *IEEE Potentials* 7, 1 (1988), 29–32. DOI: http://dx.doi.org/10.1109/45.1890
29. Pablo E. Paredes. 2016. *Pervasive Well-being Technology*. Ph.D. Dissertation. University of California, Berkeley. http://www2.eecs.berkeley.edu/Pubs/TechRpts/2016/EECS-2016-36.pdf

30. Pablo E. Paredes, Nur Al-Huda Hamdan, Dav Clark, Carrie Cai, Wendy Ju, and James A. Landay. 2017. Evaluating In-Car Movements in the Design of Mindful Commute Interventions: Exploratory Study. *Journal of medical Internet research* 19, 12 (2017), e372. DOI: http://dx.doi.org/10.2196/jmir.6983

31. Pablo E. Paredes, David Sun, and John F. Canny. 2013. Sensor-less sensing for affective computing and stress management technology. In *Proceedings of the 2013 7th International Conference on Pervasive Computing Technologies for Healthcare and Workshops, PervasiveHealth 2013*. 459–463. DOI:http://dx.doi.org/10.4108/icst.pervasivehealth.2013.252380

32. Pablo E. Paredes, Ying Zhou, Nur Al-Huda Hamdan, Stephanie Balters, Elizabeth Murnane, Wendy Ju, and James A. Landay. 2018. Just Breathe : In-Car Interventions for Guided Slow Breathing - To Appear. *Interactive, Mobile, Wearable and Ubiquitous Technologies* (2018).

33. Shwetak Patel. 2008. *Infrastructure Mediated Sensing*. Ph.D. Dissertation. Georgia Institute of Technology. http://hdl.handle.net/1853/24829

34. Andrew Pick and David Cole. 2003. Neuromuscular Dynamics and the Vehicle Steering Task. *The Dynamics of Vehicles on Roads and on Tracks* 41 (2003), 182–191. DOI:http://dx.doi.org/10.1080/00423110600882704

35. Andrew Pick and David Cole. 2007. Dynamic properties of a driver's arms holding a steering wheel. *Proceedings of the Institution of Mechanical Engineers, Part D: Journal of Automobile Engineering* 221, 12 (2007), 1475–1486. DOI: http://dx.doi.org/10.1243/09544070JAUTO460

36. Rachel L. Piferi, Keith A. Kline, Jarred Younger, and Kathleen A. Lawler. 2000. An alternative approach for achieving cardiovascular baseline: Viewing an aquatic video. *International Journal of Psychophysiology* 37, 2 (2000), 207–217. DOI: http://dx.doi.org/10.1016/S0167-8760(00)00102-1

37. Judith G. Rabkin and Elmer. L. Struening. 1976. Life events, stress, and illness. *Science* 194 (1976), 1013–1020. DOI: http://dx.doi.org/10.1126/science.790570

38. Jonathan W. Roberti, Lisa N. Harrington, and Eric A. Storch. 2006. Further Psychometric Support for the 10-Item Version of the Perceived Stress Scale. *Journal of College Counseling* 9 (2006), 135–147. DOI: http://dx.doi.org/10.1002/j.2161-1882.2006.tb00100.x

39. Jacob Rosen, Joel C. Perry, Nathan Manning, Stephen Burns, and Blake Hannaford. 2005. The human arm kinematics and dynamics during daily activities - Toward a 7 DOF upper limb powered exoskeleton. In *2005 International Conference on Advanced Robotics, ICAR '05, Proceedings*, Vol. 2005. 532–539. DOI: http://dx.doi.org/10.1109/ICAR.2005.1507460

40. James A. Russell. 1980. A Circumplex Model of Affect. *Journal of Personality & Social Psychology* 39, 6 (1980), 1161–1178. DOI:http://dx.doi.org/10.1037/h0077714

41. Peter Sainsbury and J. G. Gibson. 1954. Symptoms of Anxiety and Tension and the Accompanying Physiological Changes in the Muscular System. *Journal of Neurology, Neurosurgery & Psychiatry* 17, 3 (1954), 216–224. DOI:http://dx.doi.org/10.1136/jnnp.17.3.216

42. David Sun, Pablo E. Paredes, and John Canny. 2014. MouStress: Detecting Stress from Mouse Motion. *Proceedings of the ACM SIGCHI Conference on Human Factors in Computing Systems - CHI 2014* (2014), 61–70. DOI:http://dx.doi.org/10.1145/2556288.2557243

43. Task Force of the European Society of Cardiology and the North American Society of Pacing and Electrophysiology. 1996. Heart rate variability. Standards of measurement, physiological interpretation, and clinical use. *European Heart Journal* 17 (1996), 354–381. DOI: http://dx.doi.org/0195-668X/96/030354+28{\protect\T1\textdollar}18.00/0

44. Editha M. Van Loon, Richard S. Masters, Christopher Ring, and David B. McIntyre. 2001. Changes in Limb Stiffness Under Conditions of Mental Stress. *Journal of Motor Behavior* 33, 2 (2001), 153–164. DOI: http://dx.doi.org/10.1080/00222890109603147